

Supporting Information

Ultra-small Co₃O₄ particles embedded into N-doped carbon derived from ZIF-9 via half-pyrolysis for activating peroxymonosulfate to degrade sulfamethoxazole

Bin Su^{a,b}, Lu Zhang^{a,b}, Yifan Wang^{a,b}, Yuxin Li^{a,b}, Tianyu Zhou^{a,b}, Bo Liu^b, Wei Jiang^{a,b,*}, Linlin Liu^{b,*}, Chunhong Ma^{a,b,*}

^a College of Engineering, Jilin Normal University, Siping, 136000, P. R. China.

^b Key Laboratory of Preparation and Application of Environmental Friendly Materials (Jilin Normal University), Ministry of Education, Changchun 130103, P. R. China.

**Correspondence author*

E-mail: jiangwjlnu@163.com (Wei Jiang)

E-mail: jlsd111@163.com (Linlin Liu)

E-mail: jlspmch@163.com (Chunhong Ma)

Fax: +86-434-3290623

1. Experimental

1.1 Materials and methods

Cobalt acetate tetrahydrate ($\text{Co}(\text{CH}_3\text{COO})_2 \cdot 4\text{H}_2\text{O}$, Sinopharm Chemical Reagent Co., Ltd., AR), benzimidazole ($\text{C}_7\text{H}_6\text{N}_2$, Shanghai Macklin Biochemical Co., Ltd., AR), Ethanol (Tianjin Tiantai, AR), PMS ($2\text{KHSO}_5 \cdot \text{KHSO}_4 \cdot \text{K}_2\text{SO}_4$, Shanghai Aladdin Biochemical Technology Co., Ltd. $\geq 42\%$), SMX ($\text{C}_{10}\text{H}_{11}\text{N}_3\text{O}_3\text{S}$, Shanghai Saen Chemical Technology Co., Ltd., AR), $\text{Na}_2\text{S}_2\text{O}_3$ (Sinopharm Chemical Reagent Co., Ltd., AR), KCl (Shanghai Macklin Biochemical Co., Ltd., AR), NaHCO_3 (Tianjin Guangfu Technology Development Co., Ltd., AR), KH_2PO_4 (Beijing Beihua Fine Chemicals Co., Ltd., AR), Humic acid sodium salt ($\text{C}_9\text{H}_8\text{Na}_2\text{O}_4$, Shanghai Macklin Biochemical Co., Ltd., AR), Furfuryl alcohol ($\text{C}_5\text{H}_6\text{O}_2$, Shanghai Macklin Biochemical Co., Ltd., AR), *tert*-Butanol ($\text{C}_4\text{H}_{10}\text{O}$, Shanghai Macklin Biochemical Co., Ltd., AR), *p*-Benzoquinone ($\text{C}_6\text{H}_4\text{O}_2$, Adamas Reagent Co., Ltd., AR) were employed in this work without further purification.

1.2 Characterization

Scanning electron microscope (SEM), energy-dispersive X-ray spectroscopy (EDX, AZtecLive UltimMax100) were observed by Hitachi Regulus 8100. Transmission electron microscope (TEM) was characterized by FEI Tecnai G2 F20. Fourier transform infrared (FT-IR) spectra were acquired on a ThermoScientific Nicolet 4700 Fourier Transform Infrared Spectrometer with KBr pellet. X-ray diffraction (XRD) data were collected on a PANalytical B.V. Empyrean powder diffractometer using a $\text{Cu K}\alpha$ source ($\lambda = 1.5418 \text{ \AA}$) over the range of $2\theta = 5.0\text{--}80.0^\circ$. The sorption isotherm for N_2 was measured by using a Micromeritics ASAP 2460 analyzer with ultra-high-purity gas (99.999% purity). X-ray photoelectron spectroscopy (XPS) was recorded using Escalab 250XI X-ray electron spectrometer (VG Scientific, America). Electron paramagnetic resonance (EPR) spectra were recorded on a Bruker A300 spectrometer.

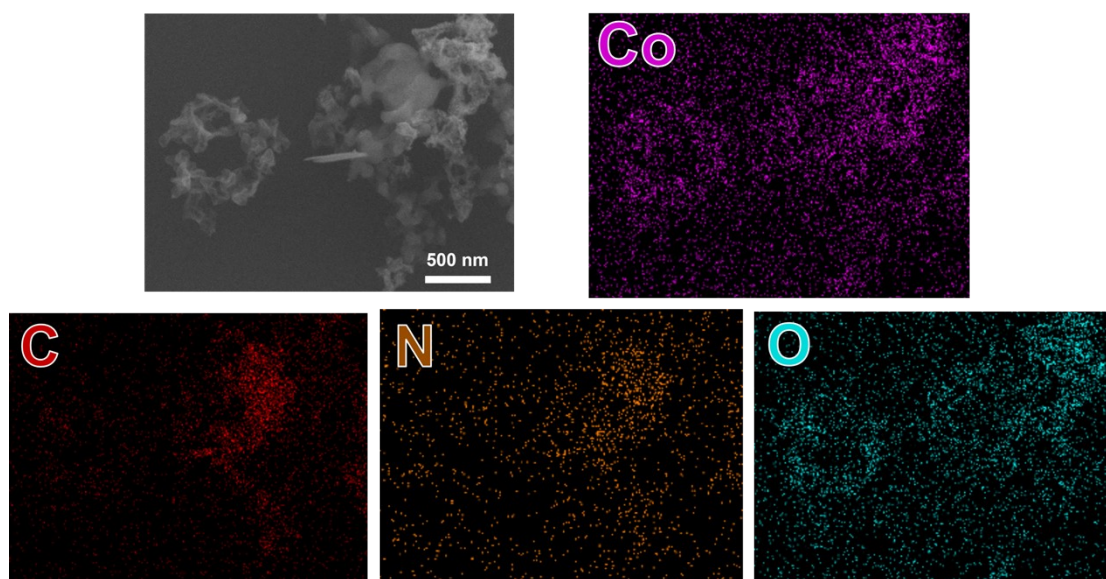


Fig. S1. The EDS-mapping of $\text{Co}_3\text{O}_4@\text{NC-350}$.

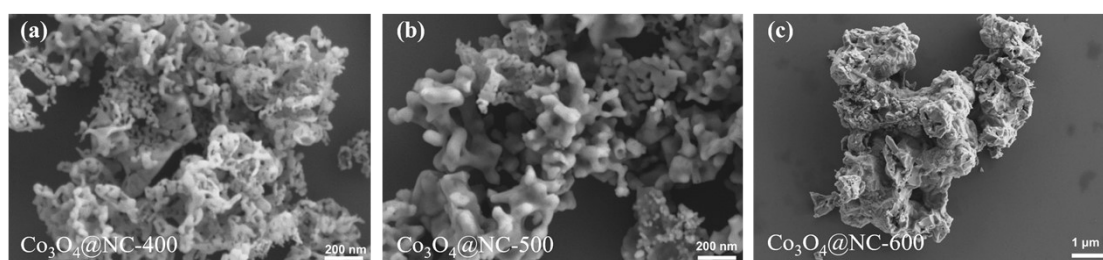


Fig. S2. The SEM images of $\text{Co}_3\text{O}_4@\text{NC-400}$, $\text{Co}_3\text{O}_4@\text{NC-500}$, $\text{Co}_3\text{O}_4@\text{NC-600}$

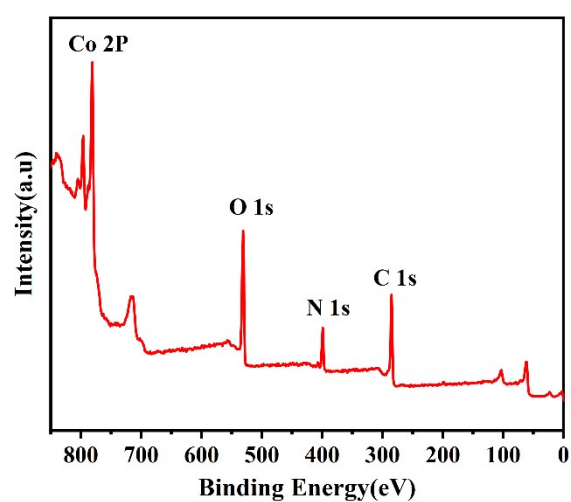


Fig. S3. The survey XPS spectrum of $\text{Co}_3\text{O}_4@\text{NC-350}$.

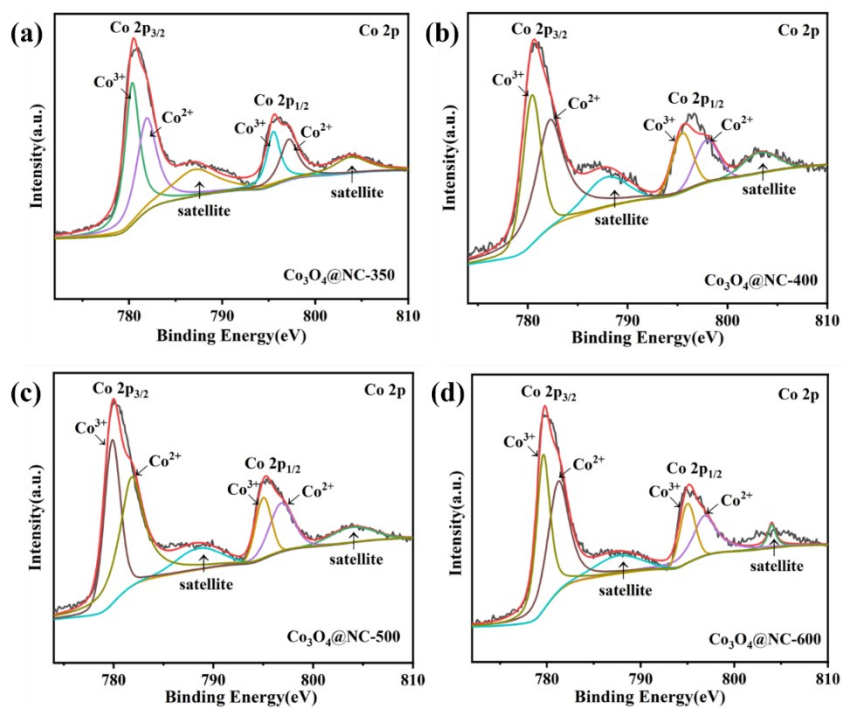


Fig. S4. The high-resolution XPS spectra of $\text{Co}_3\text{O}_4@\text{NC}$ -350, $\text{Co}_3\text{O}_4@\text{NC}$ -400, $\text{Co}_3\text{O}_4@\text{NC}$ -500, and $\text{Co}_3\text{O}_4@\text{NC}$ -600.

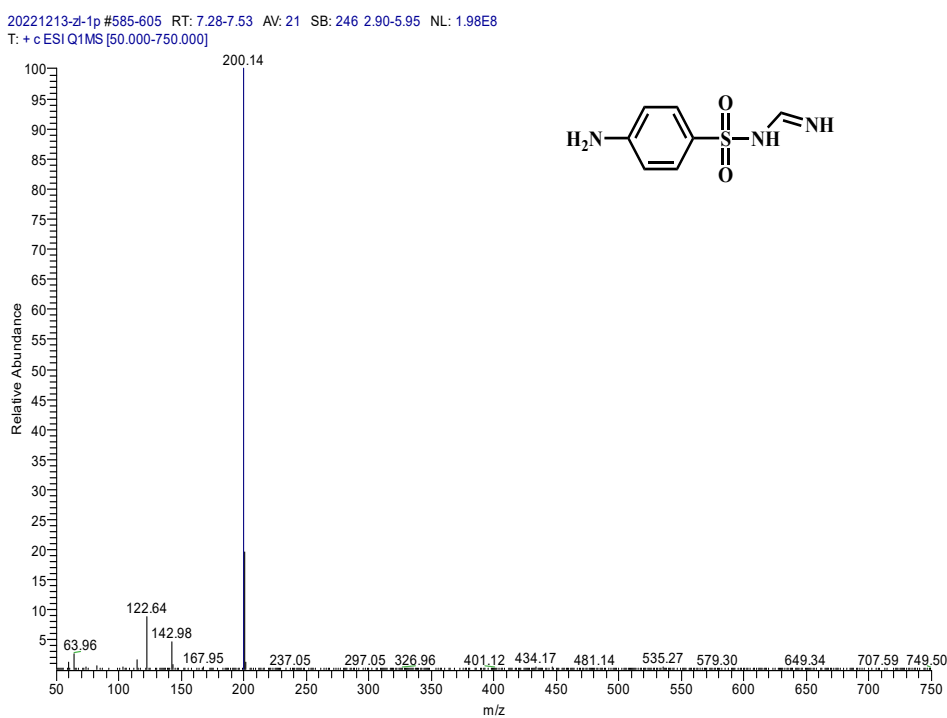


Fig. S5. Mass spectra of 200 in SMX degradation products.

20221213-zl-1p #691-716 RT: 8.60-8.91 AV: 26 SB: 27 7.68-8.01 NL: 4.02E7
T: + c ESI Q1MS [50.000-750.000]

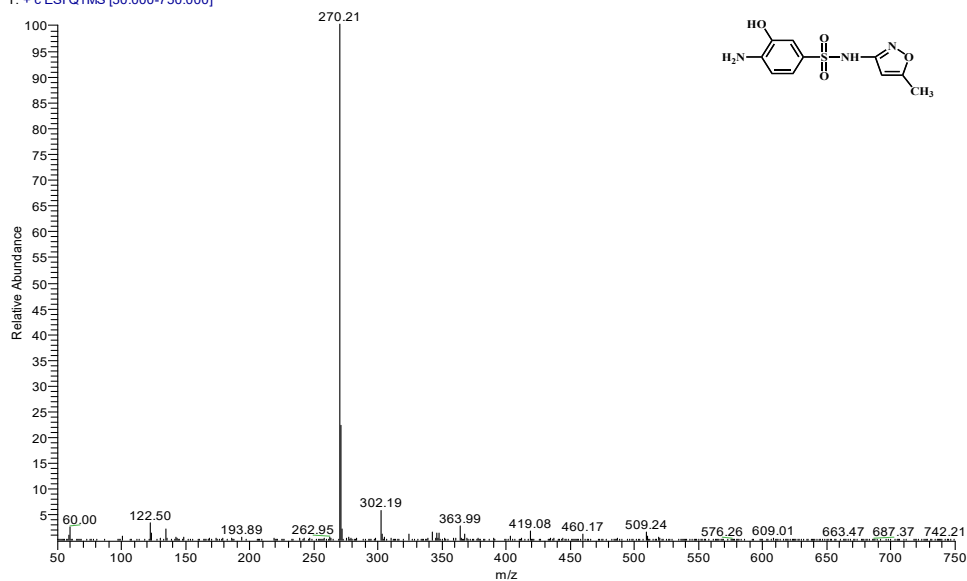


Fig. S6. Mass spectra of 270 in SMX degradation products.

20221213-zl-1p #641-658 RT: 7.98-8.19 AV: 18 SB: 27 7.68-8.01 NL: 6.32E6
T: + c ESI Q1MS [50.000-750.000]

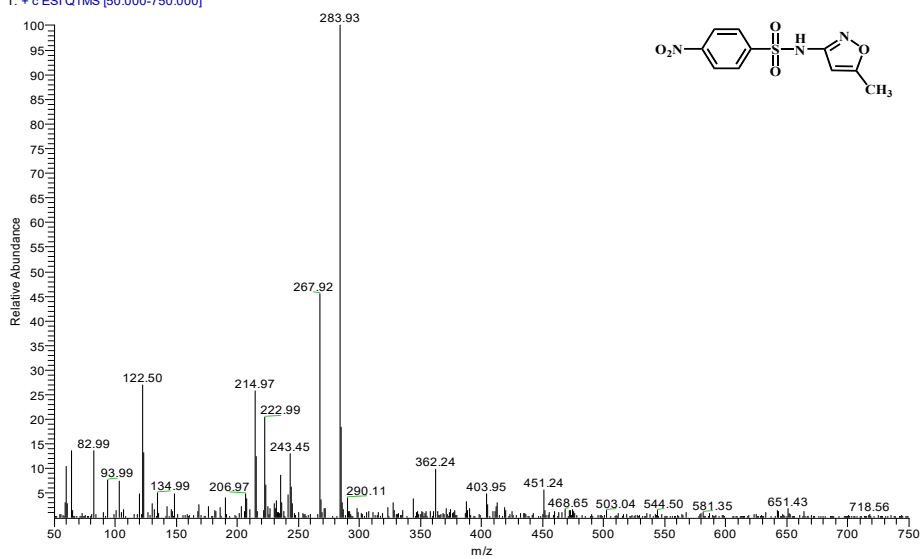


Fig. S7. Mass spectra of 284 in SMX degradation products.

20221213-zl-1p #928-942 RT: 11.56-11.73 AV: 15 SB: 27 7.68-8.01 NL: 7.84E6
T: + c ESI Q1MS [50.000-750.000]

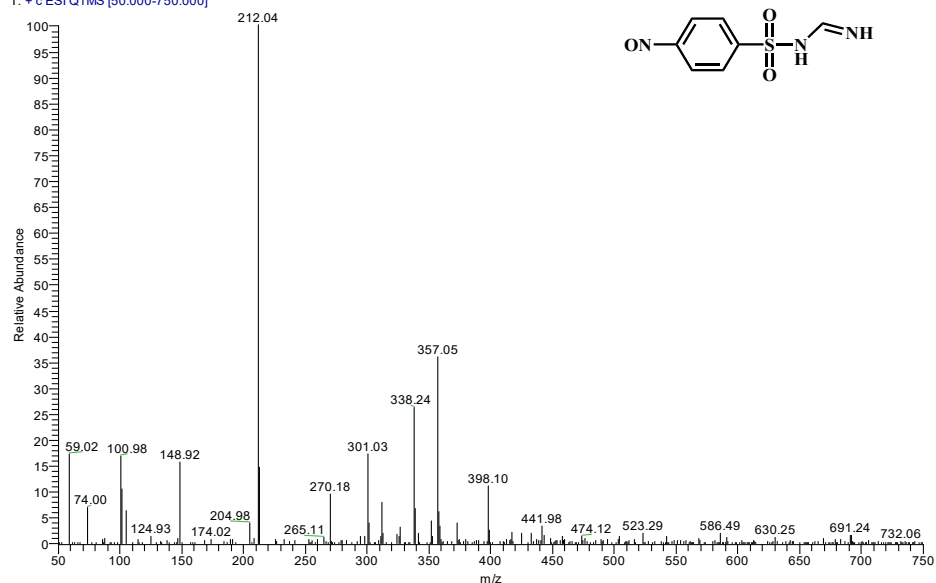


Fig. S8. Mass spectra of 212 in SMX degradation products.

20221213-zl-1p #568-579 RT: 7.07-7.21 AV: 12 SB: 246 2.90-5.95 NL: 1.95E7
T: + c ESI Q1MS [50.000-750.000]

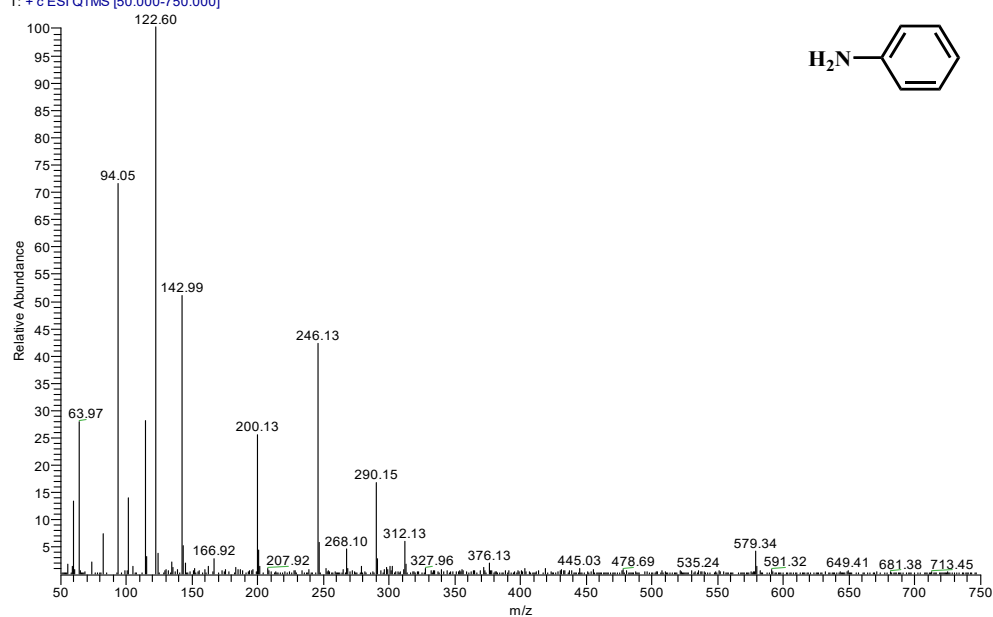


Fig. S9. Mass spectra of 94 in SMX degradation products.

20221213-zl-1p #212-226 RT: 2.64-2.81 AV: 15 SB: 155 0.32-2.24 NL: 1.09E7
T: + c ESI Q1MS [50.000-750.000]

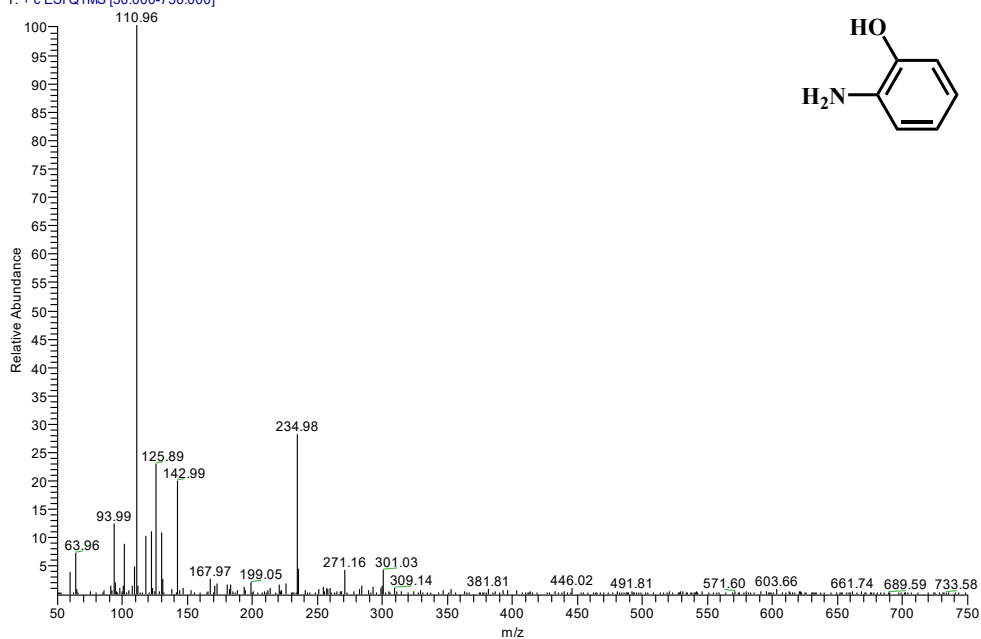


Fig. S10. Mass spectra of 110 in SMX degradation products.

20221213-zl-1p #167-174 RT: 2.08-2.16 AV: 8 SB: 11 0.03-0.16 NL: 3.96E7
T: + c ESI Q1MS [50.000-750.000]

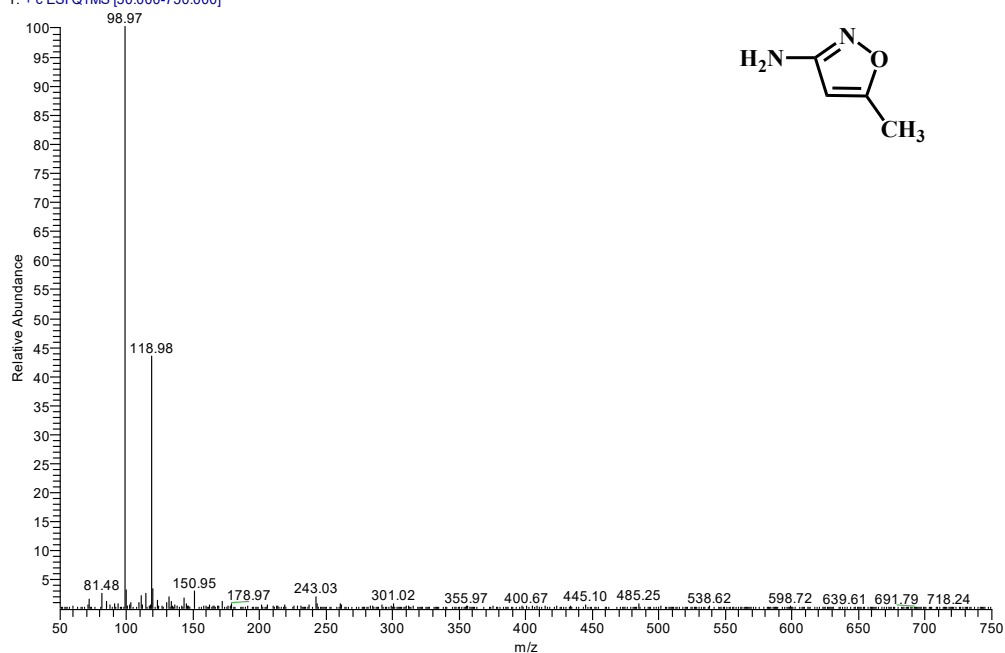


Fig. S11. Mass spectra of 99 in SMX degradation products.

20221213-z-1p #630-643 RT: 7.84-8.01 AV: 14 SB: 246 2.90-5.95 NL: 4.14E7
T: + c ESI Q1MS [50.000-750.000]

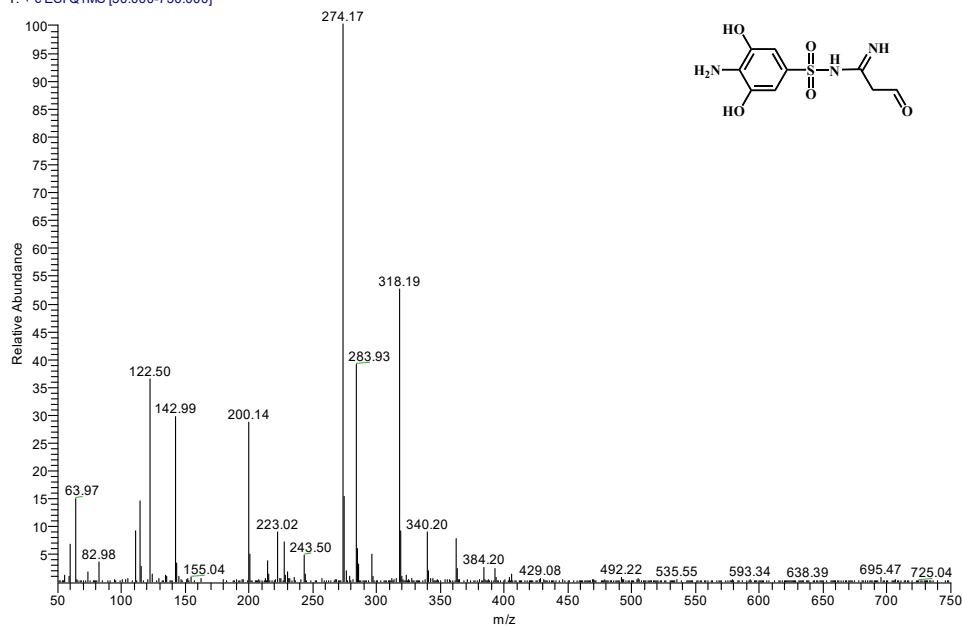


Fig. S12. Mass spectra of 274 in SMX degradation products.

20221213-z-1p #441-456 RT: 5.49-5.68 AV: 16 SB: 155 0.32-2.24 NL: 1.65E7
T: + c ESI Q1MS [50.000-750.000]

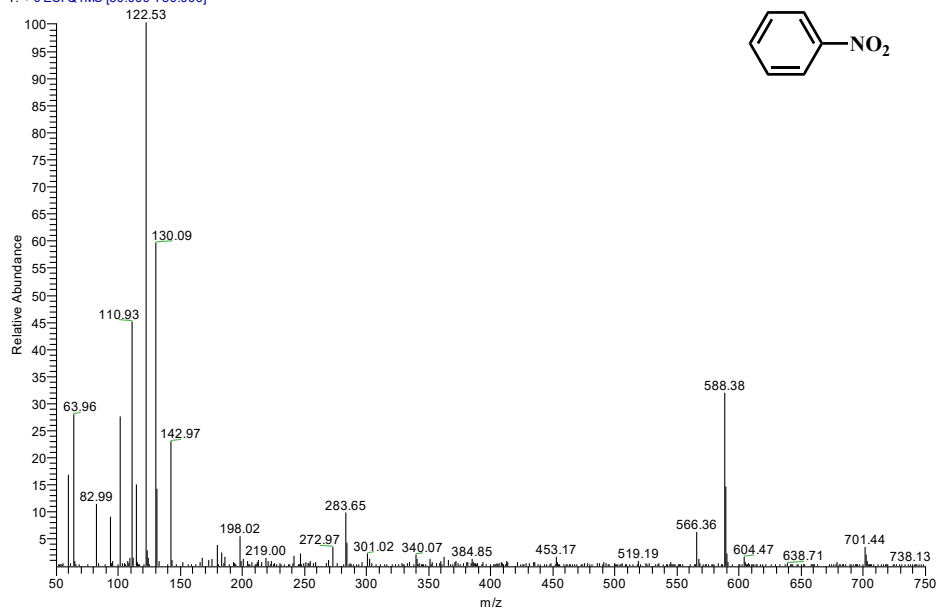


Fig. S13. Mass spectra of 123 in SMX degradation products.

20221213-z-1p #70-78 RT: 0.87-0.97 AV: 9 SB: 11 0.03-0.16 NL: 2.40E8
T: + c ESI Q1MS [50.000-750.000]

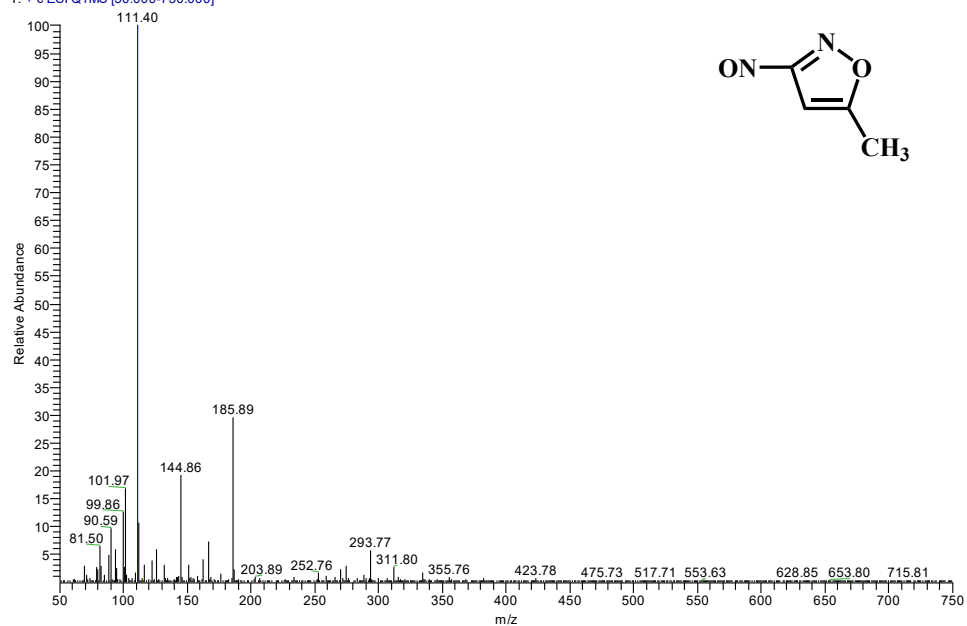


Fig. S14. Mass spectra of 111 in SMX degradation products.

20221213-z-1p #112-132 RT: 1.39-1.64 AV: 21 SB: 11 0.03-0.16 NL: 3.76E8
T: + c ESI Q1MS [50.000-750.000]

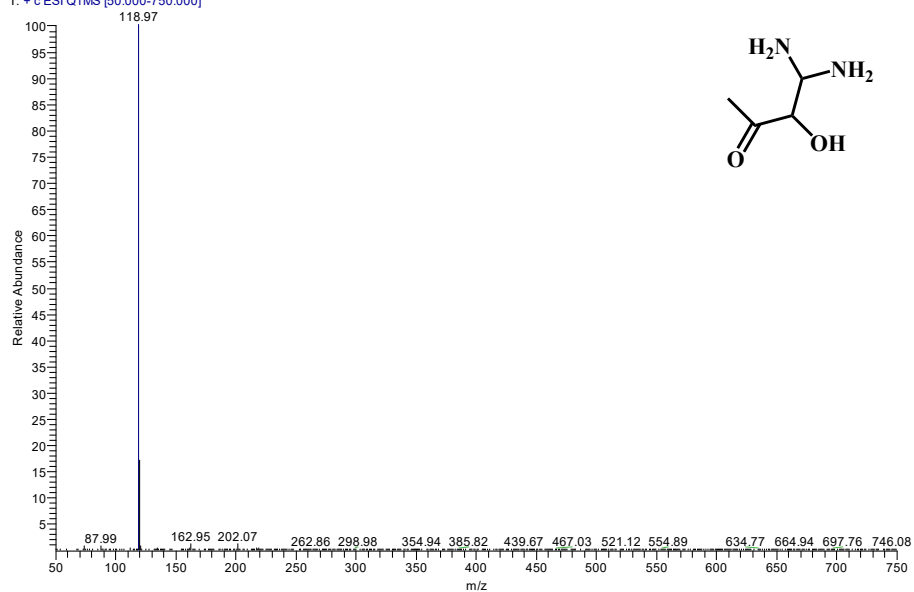


Fig. S15. Mass spectra of 119 in SMX degradation products.